INVERSE COMPTON X-RAYS FROM GIANT RADIO GALAXIES

D. TSAKIRIS [1], J.P. LEAHY [1], R.G. STROM [2], C.R. BARBER [3]

[1] *University of Manchester, Nuffield Radio Astronomy Laboratories, Jodrell Bank, Cheshire SK11 9DL, England*

[2] *Netherlands Foundation for Radio Astronomy, Radiosterrenwacht Dwingeloo, Postbus 2, NL-7990 AA Dwingeloo, The Netherlands*

[3] *University of Leicester, Department of Physics and Astronomy, Leicester, LE1 7RH, England*

1. Introduction

The X-ray radiation from inverse Compton scattering of CMB photons by the relativistic electrons in 'radio' lobes provides a direct measure of their column density at a known energy, unlike synchrotron radiation which also depends on the unknown magnetic field. Thus by combining inverse Compton and radio data we can separately determine the particle energies and field strengths, rather than having to rely on uncertain estimates like minimum energy. The predicted flux is

$$S_{IC} \propto (S_{\nu_{rad}} \nu_{rad}^{\alpha}) B^{-(\alpha+1)} (1+z)^{\alpha+3} \tag{1}$$

and strong IC signal requires high radio flux and low magnetic field, properties of giant radio galaxies. On the other hand the minimum detectable count rate, I_{min}, increases with the target size due to the larger background contribution. As a result the detectability of IC X-rays for *ROSAT* PSPC B measurements is roughly,

$$\frac{S_{IC}}{I_{min}} \propto (S_{rad} \cdot \theta \cdot z)^{1/2} (1+z)^{15/4} \tag{2}$$

assuming a spectral index of 0.75. After making detailed prediction of S_{IC} for a number of objects of the 3CR sample, the best candidates were 3C 236, 3C 326, and 4C 73.08.

R. Ekers et al. (eds.), Extragalactic Radio Sources, 256–258.

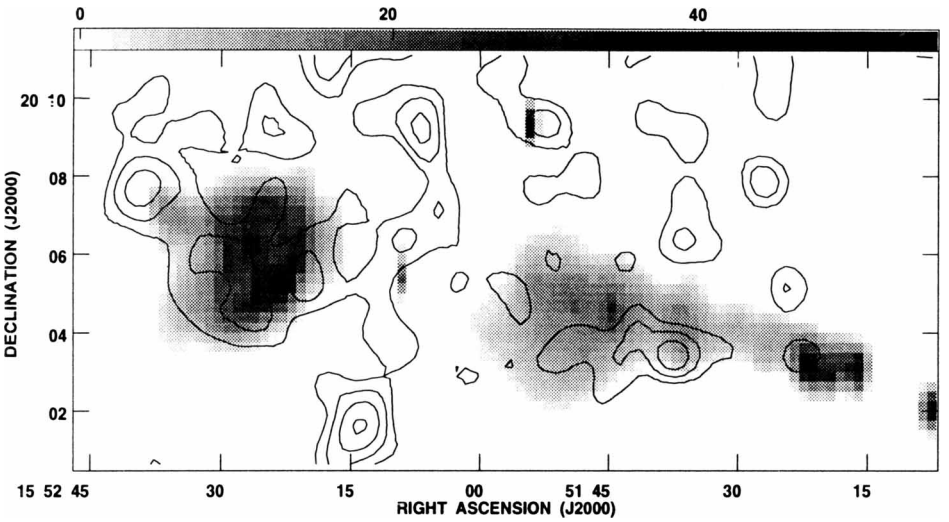

Figure 1. Smoothed X-ray image of 3C 326 in the 0.4–2 keV band overlaid on the radio image. The X-ray image was smoothed with 60×60 arcsec FWHM Gaussian. The contour levels are at 5.04×10^{-4} cts s^{-1} $arcmin^{-2}$ and increasing by factors of $\sqrt{2}$.

2. Observations and Results

We observed the targets with the *ROSAT* PSPC for about 11 ks each. The data were reduced with Dr S. Snowden's programs which model four components of non-cosmic background in the PSPC (scattered solar X-rays, particle background, 'long term enhancements', and 'short term enhancements' (STE's)). Times where our observations were affected by strong solar X-rays and STE's were excluded. To reduce confusion, we masked out all point sources detected at $> 5\sigma$, and restricted analysis to the 0.4–2 keV band. The X-ray images were compared with radio maps from the WSRT. The X-ray flux for each lobe of each object was integrated over a region defined by the outer radio contours. In each case, the average X-ray brightness was slightly higher than the average background in the field. The fluctuations in the background were substantially higher than expected from photon statistics, as expected as much of the background is contributed by individual sources below our detection threshold. To assess the significance of our detection we divided the central region of the image for each map into boxes (excluding the target) with the same number of pixels as the lobe detect cell. The standard deviation of the brightness in these background regions defines our 1σ error.

By observing giants, we avoid the problem of confusion by thermal gas associated with the host galaxy (or even from the group X-ray haloes), as the lobes of the giants are much larger. There are also low upper limits on

https://doi.org/10.1017/S0074180900080724 Published online by Cambridge University Press

entrained thermal plasma from the lack of depolarization (Strom & Willis (1980), Willis & Strom (1978), Jägers (1986)). Therefore we assumed we are seeing pure IC emission and calculated the magnetic fields required to produce the radio emission. For the regions where we lack clear detections we can give a lower limit for the magnetic field. Table 1 shows the 0.4 – 2 keV fluxes we found (using XSPEC), and Table 2 the derived magnetic fields and the comparison with the equipartition ones (with the usual assumptions and $H_0 = 75$ km s^{-1}Mpc^{-1}).

Region	3C 236	3C 326	4C 73.08
East lobe	2.9 ± 1.6	9.2 ± 1.4	12.3 ± 2.3
West lobe	9.4 ± 2.2	7.1 ± 2.1	7.3 ± 2.5

TABLE 1. Unabsorbed X-ray flux densities in units 10^{-14} erg cm^{-2} s^{-1}

Target	B_{IC} (nT) mean value	limits	B_{eq} (nT)	B_{eq}/B_{IC}
3C 236 NW lobe	0.08	(0.07 – 0.09)	0.15	1.93
SE lobe	$\geq$0.08		0.12	1.59
3C 326 East lobe	0.14	(0.13 – 0.15)	0.16	1.18
West lobe	0.16	(0.14 – 0.19)	0.16	1
4C 73.08 East lobe	0.07	(0.06 – 0.08)	0.14	2.04
West lobe	$\geq$0.11		0.14	1.29

TABLE 2. Magnetic fields derived from inverse Compton X-rays. The limits for B_{IC} derived using the 1σ errors

3. Conclusions

We have clearly detect X-ray emission from the NW lobe of 3C 236, from both lobes of 3C 326, and from the East lobe of 4C 73.08, indicating magnetic fields at the equipartition values remarkably close given the errors in both estimates. In the other two lobes the measured X-ray flux is above the background, and by 'co-adding' we obtain again a clear detection of $(10.2 \pm 2.8) \times 10^{-14}$ erg cm^{-2} s^{-1}.

References

Strom, R. G. and Willis, A. G., 1980, *Astron.Astrophys.*, **85**, 36
Jägers, W. J., PhD Thesis, The Polarization of Radio Galaxies, University of Leiden, 1986
Willis, A. G. and Strom, R. G., 1978, *Astron.Astrophys.*, **62**, 375
Snowden, S. L., Cookbook for analysis procedures, U.S.ROSAT GO Facility, 1994

https://doi.org/10.1017/S0074180900080724 Published online by Cambridge University Press